

Spin dynamics of $\text{Cd}_{1-x}\text{Mn}_x\text{Te}$ studied by muon spin relaxation and rotation

E. J. Ansaldo

Physics Department, University of Saskatchewan, Saskatoon, Canada S7N 0K3

D. R. Noakes,* J. H. Brewer, and S. R. Kreitzman

TRIUMF and Department of Physics, University of British Columbia, Vancouver, British Columbia, Canada V6T 2A6

J. K. Furdyna

Physics Department, Notre Dame University, Notre Dame, Indiana 46556

(Received 19 August 1987; revised manuscript received 26 January 1988)

The distribution and fluctuation rate of the internal magnetic field were determined in samples of $\text{Cd}_{1-x}\text{Mn}_x\text{Te}$ ($0.27 \leq x \leq 0.65$) by measurements of the relaxation rate and precession frequency of implanted positive muons in longitudinal and transverse applied fields. The results show a critical-like divergence of the μ^+ spin relaxation on approaching the spin-glass transition temperature T_g , with a critical exponent that scales with x . Relaxation rates and frequency shifts are consistent with the presence of a large hyperfine component in the μ^+ spin interaction due to superexchange. The spin dynamics is dominated by fluctuations at all temperatures. Interesting effects were also observed in the temperature range $60 < T < 250$ K which cannot be described fully by trapping or de-trapping processes and which remain a puzzling feature of the results.

I. INTRODUCTION

Interesting optical, electronic, and magnetic properties develop in II-VI semiconductors when a fraction of the cations are replaced by magnetic ions to form "diluted magnetic semiconductors" (DMS's). Most extensively studied is the zinc-blende $\text{Cd}_{1-x}\text{Mn}_x\text{Te}$ system, for which a homogeneous distribution of the substituting Mn obtains over a relatively large range of compositions $0 < x < 0.75$.¹ The $3d$ electronic levels of the Mn^{2+} ion are bound in the valence band, so that the material remains a wide-gap semiconductor, but the exchange interactions of the localized Mn ionic moments, $4.92\mu_B$ in the DMS,¹ with each other and with charge carriers result in a variety of interesting phenomena that have been reviewed in detail in Refs. 1 and 2.

The magnetic behavior of DMS's has been investigated by specific-heat, susceptibility, electron-spin resonance (ESR), and neutron-scattering techniques. The results, especially the cusp in the susceptibility at a temperature T_g and external field and remanence effects for the dilution range $0.2 < x < 0.6$ were found to be similar enough to those for the "canonical" spin glasses to warrant their inclusion in the insulating spin-glass (SG) category.^{1,2} Among these, DMS's are particularly interesting in that the SG state seems to be of a fully collective nature. The susceptibility cusp disappears at higher concentrations ($x > 0.6$), for which short-range antiferromagnetic (AF) order has been detected by means of neutron scattering.³ These results have been rationalized in terms of the lattice frustration mechanism expected in a fcc lattice with a dominant AF coupling;⁴ the coupling in this case is due to superexchange mediated by the p electrons of the host anions in a slightly distorted tetrahedral configuration.⁵ The nature of the transition and the properties of the SG

state are however not fully understood.

Due to extreme line broadening as the temperature decreases or x increases, ESR measurements are restricted to the paramagnetic region.⁶⁻⁹ Broadening and shifts of the ESR line have been ascribed to the formation and dynamics of an internal field distribution, but it was not possible to assess the origin of the field or its dynamics, for example, to state whether the line broadening is due only to the slowing down of a stable field distribution¹ or if the field distribution itself evolves with temperature. Because of the large nuclear cross section of Cd, results from neutron scattering are also sparse, showing basically that the ordering is only short range; the correlation length for $x = 0.65$ (AF case) saturates at 160 \AA (at $T = 30$ K, the transition temperature). No dynamic information has been obtained from neutron scattering, contrary to the situation in dilute metallic spin glasses, where the time ordering has been studied by neutron spin-echo techniques.¹⁰

As is well known, the dynamic depolarization of muon spins in magnetic lattices may also give direct information on the spin dynamics of the host, the SG case being very well documented for dilute systems.¹¹ We have undertaken a series of muon-spin relaxation (μSR) measurements in the DMS, and report here our results for the $\text{Cd}_{1-x}\text{Mn}_x\text{Te}$ case. Part of our zero-field results have been published¹² and Golnik *et al.* have reported on transverse field measurements in $\text{Cd}_{1-x}\text{Mn}_x\text{Te}$ samples with $x = 0.4$ and 0.6 .¹³ Since DMS are not dilute systems, and since the nature of the ordered state is far from understood from previous work, and given that the $\text{Cd}_{1-x}\text{Mn}_x\text{Te}$ system displays some departure from the canonical SG behavior in ESR,⁶ we have approached them from the point of view of a general category of random, diluted but not dilute, magnetic spin systems.

This paper is organized as follows. Section II gives experimental techniques and details of the data fitting and modeling procedures innate to the μ SR technique. A discussion of possible sites for the muon in the DMS lattice is given, including a computer calculation of the internal dipolar field distribution for the interstitial site. In Sec. III we describe the results obtained for (a) zero field (ZF) and longitudinal field (LF) (low- and high-field cases) and (b) high transverse field (TF). Interesting diffusion and trapping effects obtained at $T \geq 60$ K are discussed separately in Sec. III. To close, in Sec. IV we discuss the implications of our results in view of other work outlined above.

II. EXPERIMENTAL DETAILS, DATA ANALYSIS, AND MODELING

The basic principles and application of the μ SR techniques to the study of the spin dynamics in magnetic materials,¹⁴ particularly in spin glasses¹¹ have been sufficiently documented that only details of particular relevance to the present work will be described here. The $\text{Cd}_{1-x}\text{Mn}_x\text{Te}$ crystals studied were grown at Purdue University using a modified Bridgmann technique and are similar to those used for the previous ESR and other experiments.^{9,15} Slices of about 5 mm thickness were cleaved from crystalline ingots to form the μ SR samples, which had a crystalline $\langle 110 \rangle$ axis in the face oriented roughly perpendicular to the incident muon beam. The concentrations studied were $x = 0.275, 0.30, 0.36,$ and 0.50 in the SG region of the magnetic phase diagram, and $x = 0.65$ in the AF region. In addition, samples with $x = 0$ and 0.05 (this one doped with 10^{19} cm^{-3} Cu ions) were measured mostly for tests. The experiments were carried out using surface muons from the M15 and M20 beam lines at TRIUMF. Both channels produce pure, 100%-polarized μ^+ beams with typical momenta of about 27 MeV/c. The μ^+ beam polarization could be rotated from its usual direction parallel to the (horizontal) beam axis (conventionally defined as the z axis) into the vertical direction (hereinafter defined as the x axis) by means of the Wien velocity filter used to separate the muons from other particles in the original beam.¹⁶ The separated muon beams were focused onto the samples and stopped in about 200 mg/cm² of the sample material. Several series of runs were carried out using two different configurations. In the first series the samples were mounted in a gas-flow cryostat capable of providing very stable temperatures from 3.0 to 300 K, and experiments were carried out in small or zero applied magnetic fields to determine the ZF behavior of the muon spin dynamics. For the ZF measurements, external fields were cancelled in each of three dimensions to better than 0.1 Oe. The rest of the measurements were carried out with the samples mounted on the cold finger of a continuous-flow cryostat that provided stable (± 0.1 K) temperatures in the range of 5 to 300 K, placed in the geometrical center of a set of Helmholtz coils that could generate fields in the x - y plane of up to 200 Oe and in the z direction of up to 4.0 kOe. This is a versatile configuration that allows the measurement of ZF spectra as well as LF and TF spectra in fields up to the maximum generated by the coils.

To determine the time dependence of the muon polarization, the decay positrons were detected time differentially by up to six plastic scintillator telescopes placed pairwise along the three axes, symmetrically to the sample position taken as the origin. Most of the measurements were carried out with the z -axis counters, usually referred to as the backward-forward pair (B - F),¹⁰ the data on the other counters providing a check of, for example, the possible appearance of spurious fields.

The experimental data were accumulated as histograms, $N(t)$, of the time interval between μ^+ stop and decay e^+ detection, giving a separate $N(t)$ for each telescope. For the ZF and LF cases, using the B - F telescope pair, these time spectra have the form

$$N_{B,F}(t) = b_{B,F} + N_0^{B,F} \exp(-t/\tau) [1 \pm A_0^{B,F} G_{zz}(t)],$$

where $t=0$ is the time at which the muons stop, $b_{B,F}$ is the time-independent random background, $N_0^{B,F}$ the normalization counts at $t=0$, τ is the mean lifetime for muon decay, $A_0^{B,F}$ is the $t=0$ value of the anisotropy of the muon decay as detected by the particular detector involved, the sign (+, -) indicates the (B , F) telescope, respectively, and the function $G_{zz}(t)$ is the longitudinal muon spin depolarization function, which describes the time evolution of the muon ensemble polarization due to the interaction of the muon spin with the host. A similar expression obtains for TF histograms, where the corresponding transverse relaxation function $G_{xx}(t)$ modulates an oscillatory term $\cos(\omega_\mu t + \phi)$ describing the Larmor precession in the applied field. The backgrounds are determined experimentally from the $t < 0$ part of the time histograms. An experimental asymmetry versus time histogram is constructed as follows:

$$A(t) = \frac{B(t) - F(t)}{B(t) + F(t)},$$

where $B(t) = N_B(t) - b_B$ and $F(t) = N_F(t) - b_F$. For ideal, identical B - F telescopes the asymmetry would be $A(t) = A_0 G_{zz}(t)$, i.e., a direct measure of the depolarization function. The experimental asymmetry spectrum is actually modeled as

$$A(t) = \frac{(\alpha - 1) - (\alpha\beta + 1) A_0 G_{zz}(t)}{(\alpha\beta - 1) A_0 G_{zz}(t) - (\alpha + 1)},$$

where the instrumental parameters $\alpha = N_0^F / N_0^B$ and $\beta = A_0^F / A_0^B$ account for the different response of the B - F counter telescopes. In a typical spectrum, the background is about 1% of N_0 , $\beta \simeq 1$, $A_0 \sim 0.30$, and the parameter α depends on the particular arrangement used. The maximum asymmetry A_0 and general systematic tests are obtained from data taken on well-known samples, usually very pure Cu and Al foils. The parameter $A_b \equiv (1 - \alpha) / (1 + \alpha)$ is sometimes called the baseline, as it gives the zero-polarization value of the "raw" asymmetry $A(t)$; α was determined during the experiments from fits to both TF and LF data for each sample at several temperatures.

Several possibilities exist in modelling the depolarization function $G_{zz}(t)$.¹⁴ A well-known case is the Kubo-Toyabe function arising from a model random Gaussian

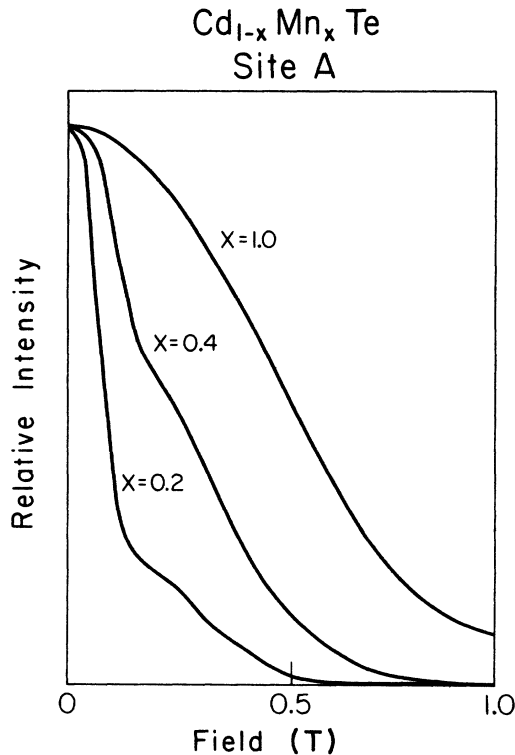


FIG. 1. Monte Carlo polycrystalline average dipolar field distribution at the tetrahedral interstitial site in which μ is surrounded by 4 Cd in CdTe, calculated for several concentrations in $\text{Cd}_{1-x}\text{Mn}_x\text{Te}$. Similar results are obtained for the second site.

distribution of internal fields acting on the muon ensemble, modified in terms of a strong-collision approximation to account for muon hopping (diffusion) and/or time fluctuation of the fields. A special form has been introduced by Uemura *et al.*¹¹ for the case of the dilute spin glasses, which is in principle applicable to random systems in general, and has recently been shown to reproduce the data well for the amorphous spin glasses $\text{Pd}_{75}\text{Fe}_5\text{Si}_{20}$ and $\text{Pd}_{75}\text{Fe}_5\text{P}_{20}$.¹⁷ Despite its basic importance in μSR , the SG function will not be given here because, as discussed later, the experimental depolarization functions found for the $\text{Cd}_{1-x}\text{Mn}_x\text{Te}$ system were of a simple exponential relaxation shape $G_{zz}(t) = \exp(-\lambda t)$. An exponential shape obtains in the limit of fast fluctuations for a classical distribution of fields and basically yields only limited information on such fields, as the relaxation parameter $\lambda = \omega_0^2 \tau_c$ contains both the magnitude of the local mean field ω_0 / γ_μ and its fluctuation rate $1/\tau_c$.

Further insight into the field distributions expected in different crystalline lattices may be gained by a numerical-modeling procedure discussed in detail in Ref. 18. As a positive impurity of negligible size, the muon is assumed to reside at an interstitial site with relatively low electron charge density. There are two such sites (both with tetrahedral symmetry) in the zinc-blende structure. Figure 1 shows the calculated instantaneous ("snapshot") Monte Carlo average of the dipolar fields due to the Mn ionic moments that randomly replace Cd ions in $\text{Cd}_{1-x}\text{Mn}_x\text{Te}$, performed on a cluster of more than 400

ions centered on the interstitial site with four Cd nearest neighbors (NN) in the CdTe lattice. The effect of the nuclear dipoles can be neglected. The distribution obtained departs from a simple Gaussian form for $x < 0.5$, as observed before,¹⁸ and has a rms width of ≤ 0.5 T for the concentration $x = 0.4$. This provides a starting point in estimating the (minimum) static distribution of internal fields at the muon site due to dipolar interactions alone, which therefore should be noticeably affected by the applied field of 0.4 T available in our spectrometer, if the fluctuation rates are lower than approximately 50 MHz.

III. RESULTS

A. Zero and longitudinal field

The shape of the asymmetry histogram was similar for the different compositions and is shown for the case $x = 0.5$ in Fig. 2. The main features of the data are an initial asymmetry A_0 that is slightly (typically 15%) smaller than that obtained for the calibration Cu and Al samples, and a rapid decay of the signal within the first microsecond to a slowly varying signal within the 10 μs total time measured. A missing fraction of the initial asymmetry in insulators is normally due to the formation of muonium (Mu) atoms, which if present, aside from the small reduction of the experimental A_0 observed, play no role in the present results. No direct evidence was found for Mu formation in either pure CdTe or the $\text{Cd}_{1-x}\text{Mn}_x\text{Te}$ samples. The depolarization signal could not be fitted consistently (i.e., all temperatures for the same x) using the full SG relaxation function discussed, for example, in Ref. 11; in those individual cases yielding a good fit (in terms of χ^2 values) unphysical values were obtained for the fitted parameters. By contrast, consistent fits with very good χ^2 values were obtained in all cases by assuming two signals in the data: a dominant one with a typical asymmetry of 0.25, exhibiting relatively fast exponential decay, superimposed on a slowly relaxing background signal which could be fitted to a dynamic Kubo-Toyabe form in the ZF field case and to an exponential with very small relaxation constant in the LF and TF cases. The asymmetry of the second signal was typically less than 0.05. We attribute this background signal to a small fraction of the muons (at most 15%) stopping in nonmagnetic sites, mostly in the Cu and Al sample backings but not excluding the possibility of a small fraction of muons residing at diamagnetic sites in the $\text{Cd}_{1-x}\text{Mn}_x\text{Te}$ lattice. This is consistent with the fact that, in order to insure good thermal contact with the cold finger, there were some openings left in between the flat ovoidal slices that constituted the sample. In addition, the relaxation constant obtained for the Cu-backed samples in ZF followed the well-known temperature dependence for that metal, while that for the Al-backed samples was T independent and both were rendered flat (i.e., decoupled) by a 50-Oe LF. An exponential relaxation function described the main signal very well in all cases; no other assumptions regarding the shape of $G_{zz}(t)$ were required to account for the experimental results. The important experimental quantity extracted from the

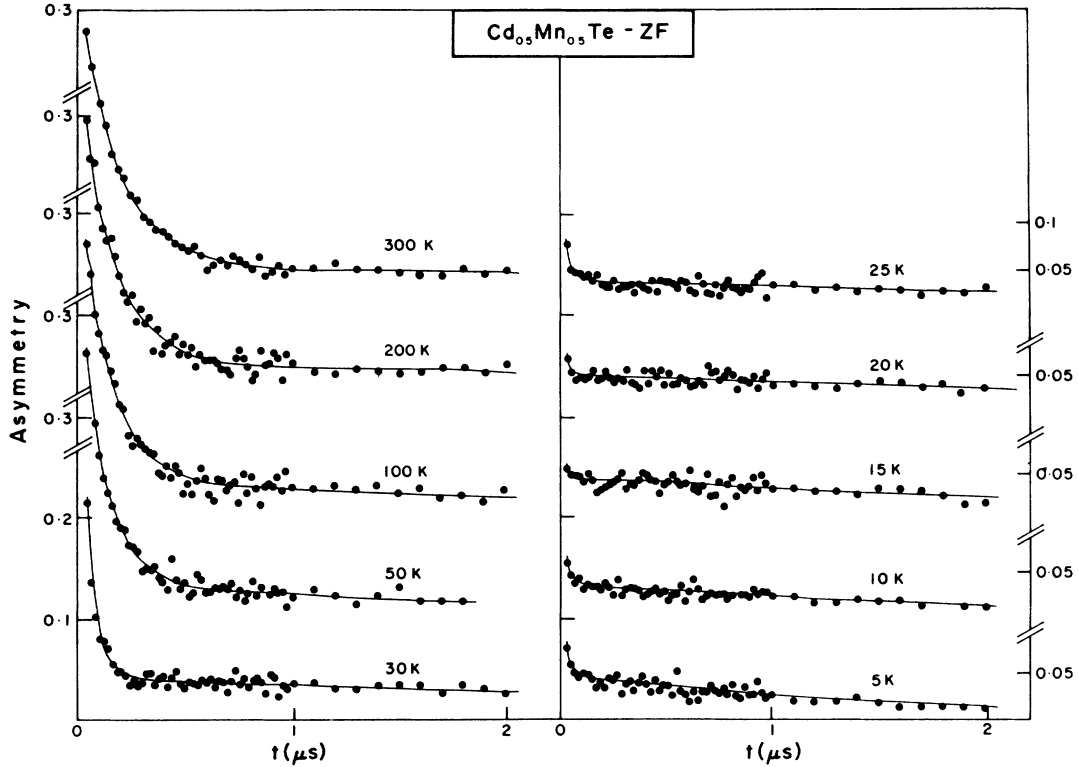


FIG. 2. Example of the temperature evolution of the asymmetry $A(t)$ obtained for $\text{Cd}_{0.5}\text{Mn}_{0.5}\text{Te}$. The solid lines are the results of fits described in the text.

data is thus the relaxation parameter λ , which was then measured as a function of x , T , and the magnitude of the LF.

The temperature dependence $\lambda(T)$ is shown in Fig. 3 for several concentrations x . The most striking features of the data are (a) the apparent divergence of $\lambda(T)$ as the temperature is reduced from about 100 K in the paramagnetic region towards an x -dependent "transition" temperature; and (b) the almost total disappearance of the signal below that temperature. The "transition" temperature extrapolated from the diverging behavior of $\lambda(T)$ and the sudden drop in asymmetry of the main μSR signal agreed (to within 1 K) with the susceptibility cusp temperature for the same x , i.e., the temperature previously identified as T_g for the transition to SG ordering. It is interesting to note that, within experimental errors, the same values of $\lambda(T)$ were obtained in a 50-Oe LF, for both zero-field-cooled and field-cooled cycles. Below T_g the main signal displayed a very small asymmetry, less than 0.04 in all cases, and its relaxation parameter could not be extracted with any accuracy.

Except for an unavoidable shift in the baseline and thus uncertainty in the initial asymmetry, no appreciable change was observed in the main signal between ZF and the maximum available LF for several test cases measured above and below T_g (as low as 5 K). As expected from its proposed origin, the background signal remains the same above and below T_g and is fully decoupled by a LF greater than 50 Oe.

A high-temperature "plateau" in $\lambda(T)$, is also apparent near 300 K, varying from $\lambda(300 \text{ K}) \sim 4.5 \mu\text{s}^{-1}$ for

$x = 0.65$ to $\lambda(300 \text{ K}) = 13.5 \mu\text{s}^{-1}$ for $x = 0.275$. In addition to the divergence on approaching T_g and the high-temperature plateau in $\lambda(T)$, which are due to the interaction of the muon spins with the Mn^{2+} ensemble, a drastic change in the relaxation function was observed at low concentrations $x \lesssim 0.36$ for temperatures $60 < T < 250 \text{ K}$. In this "dip" region, the relaxation rate for the great majority of the muons decreases to a small value comparable to that obtained for pure CdTe crystals. One might be tempted to explain this dramatic effect in terms of a trapping or detrapping mechanism whereby the muons would fall into diamagnetic traps at around 90 K with subsequent fast detrapping above 250 K; however, as discussed below, this simple model is inconsistent with the data. No orientation dependence of the measured $\lambda(t)$ was observed, either by rotating the crystals or by powdering the $x = 0.50$ sample to get a polycrystalline average.

B. Transverse field

A less exhaustive series of measurements was carried out in a transverse field of 0.33 T in quest of further insight into the origin of the internal field distribution and the muon state responsible for the dip in the ZF relaxation rate discussed above. The results shown as Fourier transforms in Fig. 4 were in agreement with those of Golnik *et al.*¹³ In addition to the unshifted signal due mostly to the sample holders, a distribution of negative frequency shifts is observed. The magnitude of the shifts increase linearly with the applied field and increase with decreasing temperature. In fitting the TF data more than

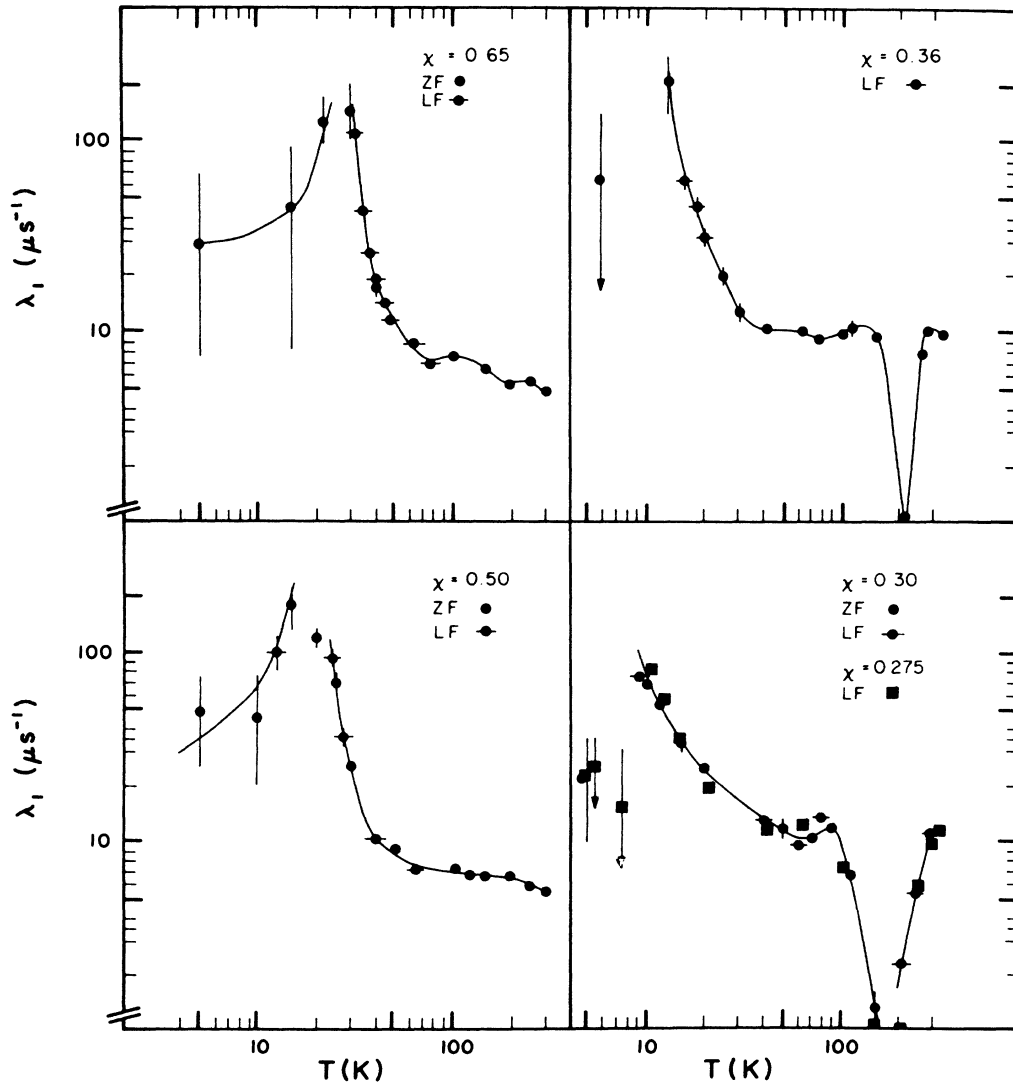


FIG. 3. Temperature dependence of the exponential relaxation rate of the main signal for several compositions x as labeled. The values below T_g are subject to large errors due to the vanishing effective anisotropy of the signal there, and are shown only for illustrative purposes.

two signals were necessary above 90 K, i.e., in the region of the dip in the ZF relaxation rate. Figure 5 shows the relative frequency shift of the dominant signal relative to the background signal as an indication of temperature dependence of the centroid of the internal field distribution. A striking feature of the shift data is the existence of a minimum, for example, at $T = 200$ K for $x = 0.36$, with features similar to those of the relaxation rate. As is apparent to the eye in the Fourier-transformed data of Fig. 4, the field distribution becomes quite narrow for temperatures around the minimum, where it becomes indistinguishable from the background signal, reappearing again as a shifted distribution at higher temperatures. Again, near and below the transition temperature T_g only the background signal can be discerned in the data.

IV. SUMMARY AND CONCLUSIONS

For the purpose of this discussion it is convenient to divide the data in four temperature ranges, namely (a)

$T < T_g$, the “low-temperature” regime; (b) $T_g < T \leq 60$ K, the “critical” region or “paramagnetic” regime; (c) the “dip” region, roughly $80 \text{ K} < T \leq 250 \text{ K}$; and (d) the “high-temperature” region, $T \approx 300 \text{ K}$. As discussed above, most of the signal disappears at low temperatures, below T_g . This behavior is similar to that of the canonical spin glasses, where it has been shown to be due to the onset of a quasistatic distribution of fields in the ordered state. In that case, however, a fraction $\frac{1}{3}$ of the asymmetry remains and is gradually relaxed by the “dynamic” components of the fields, which can thus be separated from the “static” component.^{10,17} In the present DMS case, however, the anisotropy decays to a value below $\frac{1}{3}A_0$ in less than 20 ns, implying that fast fluctuations persist at low temperatures and thus that the “spin freezing” (if any) is far from complete in the DMS at temperatures down to 5 K. The relaxation rate $\lambda(T)$ for $T \geq T_g$ displays critical behavior, i.e., a power-law behavior $\lambda \sim \tau^{-\alpha}$ in the reduced temperature variable

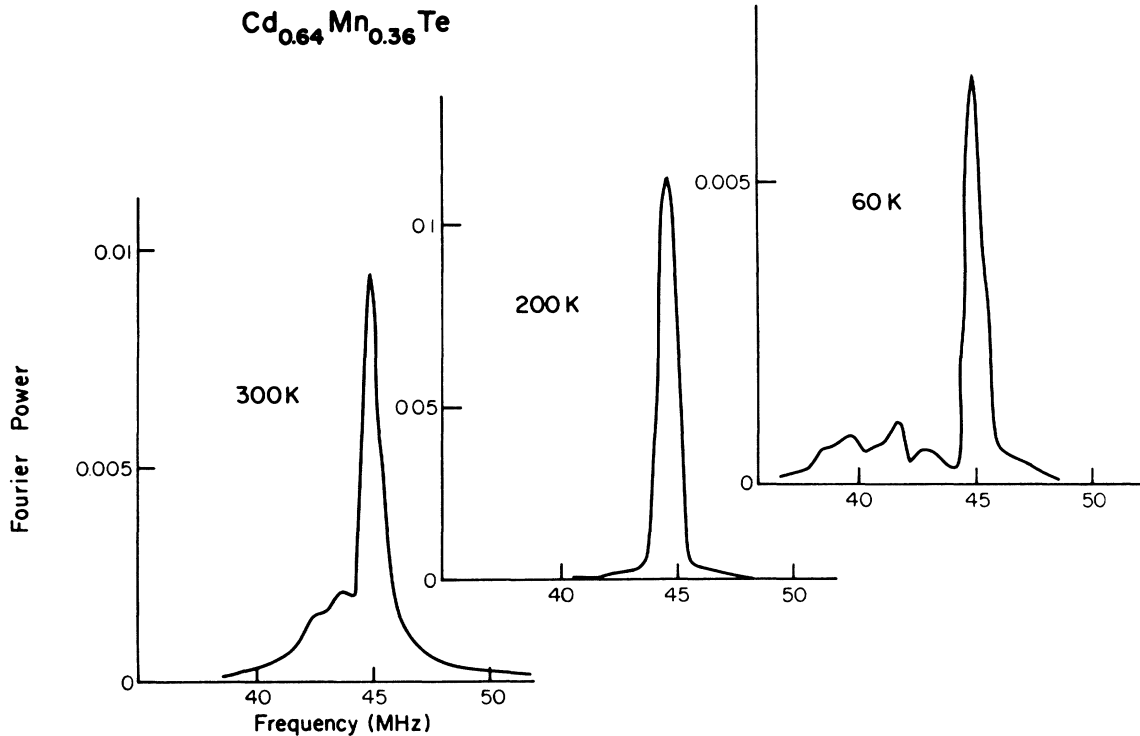


FIG. 4. Example of Fourier transforms of $A(t)$ obtained in TF geometry at 0.33 T. Only the initial 500 ns of data were used to be able to display both the shifted, broad signal (high-relaxation rate) and the unshifted background signal (unrelaxed) simultaneously. For clarity of the diagram, the fine details of the Fourier spectrum were smoothed out in the line drawing.

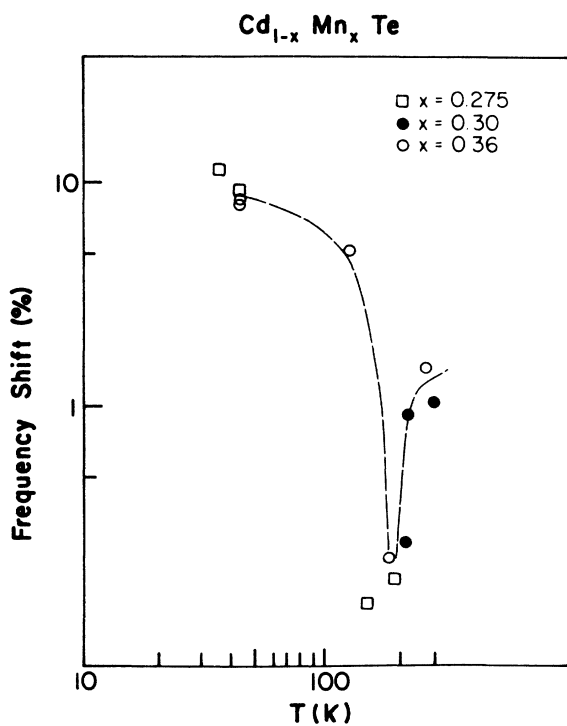


FIG. 5. Temperature dependence of the magnitude of the frequency shifts (in percent) obtained for the dominant signal in fits to two or three signals of the TF data.

$\tau = T/T_g - 1$, as shown in Fig. 6, which extends up to $\tau \approx 10$ at low concentrations. The exponent α obtained from the data of Fig. 6 is shown in Fig. 7 as a function of composition x and transition temperature T_g . It is interesting to note that α increases with concentration from $\alpha \approx 0.7$ for $x = 0.3$ to $\alpha \approx 1.4$ for $x \approx 0.5$ in the SG region and has an intermediate value (~ 0.93) in the AF case.

In Fig. 7 is also displayed the composition dependence of $\lambda(300 \text{ K})$, the relaxation rate in the high-temperature limit, which decreases with concentration from about $13.5 \mu\text{s}^{-1}$ at $x = 0.275$ to a "saturation" value of $5.5 \rightarrow 4.5 \mu\text{s}^{-1}$ for $x = 0.5 \rightarrow 0.65$. Assuming that at 300 K the high-temperature limit of the exchange narrowing effect has been reached¹⁹ this means that the exchange frequency ω_{ex} increases with increasing concentration, almost linearly in our measurements, to a saturation value at $x \geq 0.50$. Insofar as the muons probe the spin dynamics of the host, our main experimental results that (a) fluctuations persist below the transition and the spin freezing is far from complete, (b) critical behavior with concentration-dependent exponent, and (c) concentration-dependent exchange narrowing indicate that DMS's are fairly different from the conical spin glasses¹¹ or from insulating antiferromagnets.¹⁴ We present our results as experimental evidence that should be incorporated into any attempts of modeling the DMS behavior. Similar results and conclusions were reached in ESR experiments,^{6-9,15} where the extreme line broadening precluded measurements around the transi-

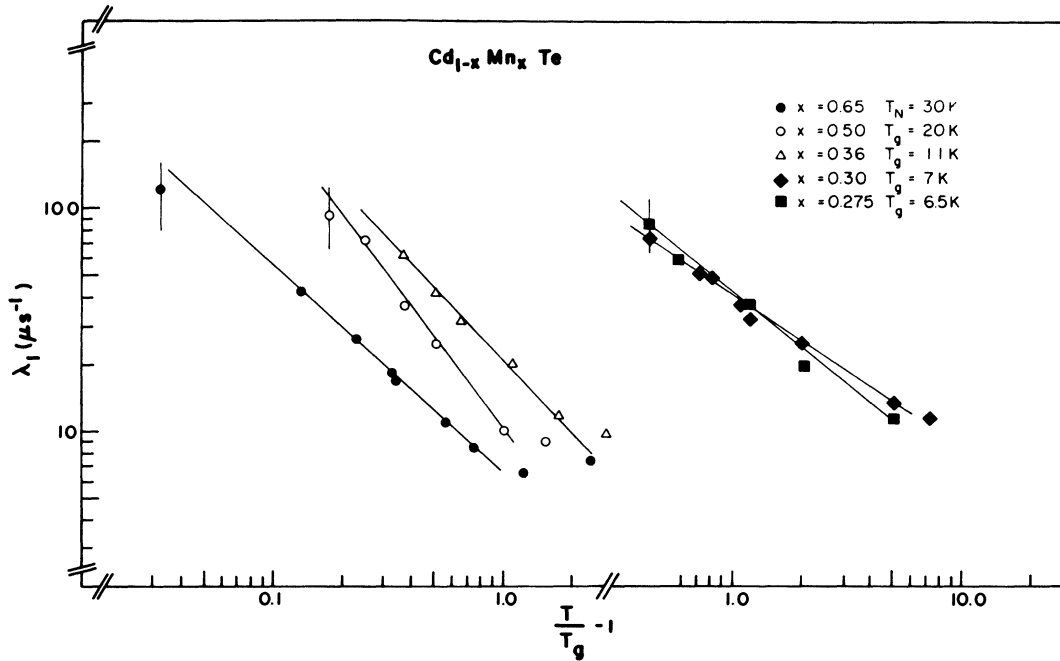


FIG. 6. Relaxation rates λ in the paramagnetic region showing the critical behavior. The transition temperatures listed were obtained from the λ data of Fig. 2 and are in good agreement with the cusp T_g for the given compositions.

tion temperature. A critical behavior was, however, observed by Oseroff,⁶ who obtained $\alpha \approx 1.5$ for $x \geq 0.3$. This should be considered in good agreement with our results, given the large extrapolation required in the ESR case. Note, however, that the μSR critical exponents are obtained at zero field. A more recent systematic ESR study has also shown considerable departure from canonical spin-glass behavior.¹⁵ At high temperatures the con-

centration dependence of the (Lorentzian) linewidth is stronger than predicted by exchange narrowing and cannot be explained by dipolar anisotropy alone in the $\text{Cd}_{1-x}\text{Mn}_x\text{Te}$ case. At low temperatures the ESR lineshape becomes non-Lorentzian, which could not be explained for example by a Kubo-Toyabe approach. The required phenomenological internal field would have to be non-Gaussian and shifted from zero mean.¹⁵

An attempt to describe the microscopic origin of the fields experienced by the μ^+ can be pursued as follows. In a perfect CdTe lattice there are two large interstitial openings that the positive muon may occupy, surrounded tetrahedrally by four Cd or Te ions, respectively, at a distance of 2.607 Å. For $x \geq 0.5$, when Cd ions are replaced by Mn, at least half of the muons will have one or more Mn ions as next neighbors. The distribution of dipolar fields due to the random distribution of the interstitial muons in a lattice in which the substituted Mn ions are themselves assumed randomly distributed has been shown in Fig. 1. The strength of such dipolar fields alone is not sufficient to account for our results. If we assume that the fluctuations of the muon spin system are driven by those of the Mn^{2+} spins, given in turn by the exchange frequency which can be estimated from the known values of the exchange constants ($\hbar\omega_{\text{ex}} \approx J_{\text{NN}} \approx k_B \times 10 \text{ K}$) (Ref. 1) to be of order $\omega_{\text{ex}} \approx 9 \times 10^{11} \text{ s}^{-1}$, the values of $\lambda(300 \text{ K})$ (Fig. 7) cannot be due to just the dipolar interaction. If, conversely, we assume that only an isotropic hyperfine interaction is present, we obtain a hyperfine-constant value $A/\hbar \approx 600 \text{ MHz}$, similar in value to that obtained for muonium in semiconductors. Since formation of neutral muonium in CdTe is not a major effect, we are led to conclude that the muon spin in the $\text{Cd}_{1-x}\text{Mn}_x\text{Te}$ lattices is affected both by dipolar interactions and by the hyperfine

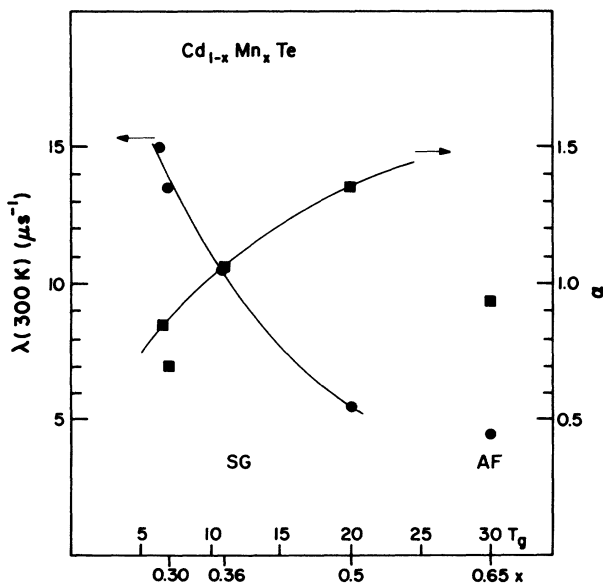


FIG. 7. Combined plot of the T_g - x dependence of the critical exponent α (squares) (right-hand scale) and the high-temperature limit $\lambda(300 \text{ K})$ (circles) (left-hand scale).

interaction due to the interstitial unpaired electronic spin density that plays an essential role in the magnetic properties of DMS. Such interactions with electrons and dipole moments in the random system manifest themselves as the shifted precession frequency distributions of Fig. 4 in an applied field (TF experiments). The magnitude of the interactions and their fairly rapid fluctuations prevent the observation of anisotropy effects or decoupling effects in applied fields below 1 T in longitudinal field cases.

The above conclusions are valid even if the μ^+ occupies sites other than the assumed tetrahedral interstitials. The magnitude of the hyperfine fields detected could, on the other hand, imply that perhaps the μ^+ in $\text{Cd}_{1-x}\text{Mn}_x\text{Te}$ forms $\text{Cd}-\mu^+-\text{Te}$ or $\text{Mn}-\mu^+-\text{Te}$ bonds along preferred crystalline directions, as in the case for Si and III-V semiconductors.²⁰ In such cases the μ^+ would be in a paramagnetic state, i.e., muonium atom, but, contrary to Si and other semiconductors, no evidence was found for Mu formation in CdTe during this and previous μSR work.^{12,13}

The dip region, i.e., the dramatic decrease in $\lambda(T)$ at $60 \leq T \leq 250$ K is not amenable to a straightforward description in terms of diffusion trapping processes. A

similar minimum in metallic systems indicates trapping at, for example, vacancies as the muons become mobile as the temperature is raised, with subsequent detrapping at higher temperatures. There are, however, definite difficulties in applying such a picture to the present situation. The magnitude of the change in $\lambda(T)$ implies that a large majority of the muons would need to reach non-magnetic traps (i.e., negligible relaxation rate) within a few nanoseconds time, i.e., very fast motion and/or a large number of trapping sites. An order of magnitude of $\leq 10 \mu\text{s}^{-1}$ for the hop rate of the muons could be extracted from measurements on the Cu-doped sample, for which the $G_{zz}(t)$ displayed a definite nonstatic shape in the 100–200-K range.

Similarly the muon motion is too slow to explain the decrease in $\lambda(T)$ as a motional narrowing effect, and the $\lambda(T)$ minimum is not apparent for $x \geq 0.4$. The motional narrowing in that case is dominated by the spin fluctuations. We are, therefore, left with a puzzle, since the defect and impurity concentration levels in our samples are very low (i.e., 10^{17} cm^{-3}) and the Mn^{2+} distribution is spatially quite homogeneous.^{1,7,9,15}

*Present address: Chalk River National Laboratory, AECL, Chalk River, Ontario, Canada K0J 1J0.

¹J. K. Furdyna, *J. Appl. Phys.* **61**, 3526 (1987), and previous references therein.

²R. R. Gałazka, S. Nagata, and P. H. Keesom, *Phys. Rev. B* **22**, 3344 (1980).

³U. Steigenberger, B. Lebech, and R. R. Gałazka, *J. Magn. Magn. Mater.* **52-57**, 1285 (1986); T. M. Holden, G. Dolling, V. F. Sears, J. K. Furdyna, and W. Giriat, *Phys. Rev. B* **26**, 5074 (1982).

⁴L. DeSeeze, *J. Phys.* **10**, 1353 (1977).

⁵J. Spałek, A. Lewicki, Z. Tarnawski, J. K. Furdyna, R. R. Gałazka, and F. Obuszko, *Phys. Rev. B* **33**, 3407 (1986).

⁶S. B. Oseroff, *Phys. Rev. B* **25**, 6584 (1982).

⁷D. J. Webb, S. M. Bhagat, and J. K. Furdyna, *J. Appl. Phys.* **55**, 2310 (1984).

⁸H. A. Sayad and S. M. Bhagat, *Phys. Rev. B* **31**, 591 (1985).

⁹R. E. Kremmer and J. K. Furdyna, *J. Magn. Magn. Mater.* **40**, 185 (1983); *Phys. Rev. B* **31**, 1 (1985).

¹⁰F. Mezei and D. P. Murani, *J. Magn. Magn. Mater.* **14**, 211 (1979).

¹¹Y. J. Uemura, T. Yamazaki, D. R. Harshman, M. Senba, and

E. J. Ansaldo, *Phys. Rev. B* **31**, 546 (1985), and references therein; R. H. Heffner, M. Leon, M. Schillaci, S. A. Dodds, G. A. Gist, D. E. MacLaughlin, J. A. Mydosh, and G. J. Nieuwenhuys, *J. Appl. Phys.* **55**, 1703 (1984).

¹²E. J. Ansaldo, D. R. Noakes, R. Keitel, S. R. Kreitzman, J. H. Brewer, and J. K. Furdyna, *Phys. Lett.* **A120**, 483 (1987).

¹³A. Golnik, E. Albert, M. Hanna, E. Westhauser, A. Weidinger, and E. Recknagel, *Hyperfine Interact.* **32**, 375 (1986).

¹⁴A. Schenk, *Muon Spin Rotation Spectroscopy—Principles and Applications to Solid State Physics* (Hilger, Bristol, 1985).

¹⁵N. Samarth, Ph.D. thesis, Purdue University, 1986 (unpublished).

¹⁶J. L. Beveridge, J. Doornbos, D. M. Garner, R. Keitel, and J. T. Worden, *Hyperfine Interact.* **32**, 907 (1986).

¹⁷J. H. Brewer, D. P. Spencer, C. Y. Huang, Y. J. Uemura, and H. J. Chen, *Hyperfine Interact.* **32**, 381 (1986).

¹⁸D. R. Noakes, *Hyperfine Interact.* **32**, 57 (1986).

¹⁹V. Jaccarino, in *Magnetism*, edited by G. T. Rado and H. Suhl (Academic, New York, 1965), Vol. IIA, p. 307.

²⁰R. F. Kiefl, M. Celio, T. Estle, E. J. Ansaldo, G. M. Luke, S. R. Kreitzman, J. H. Brewer, and D. R. Noakes, *Phys. Rev. Lett.* **58**, 1780 (1987).